Synthetic and Systems Biotechnology 9 (2024) 209–216

Contents lists available at ScienceDirect

Synthetic and Systems Biotechnology

journal homepage: www.keaipublishing.com/en/journals/synthetic-and-systems-biotechnology

Short Communication

A CRISPR/Cas9-based visual toolkit enabling multiplex integration at specific genomic loci in *Aspergillus niger*

Yangyang Li [a,b,c], Cen Li [e], Yishan Fu [a,b,c], Quan Zhang [f], Jianing Ma [g], Jingwen Zhou [a,b,c,d], Jianghua Li [a,b,c], Guocheng Du [a,b,c], Song Liu [a,b,c,*]

[a] National Engineering Research Center for Cereal Fermentation and Food Biomanufacturing, Jiangnan University, Wuxi, 214122, China
[b] Science Center for Future Foods, Jiangnan University, Wuxi, 214122, China
[c] School of Biotechnology, Jiangnan University, 1800 Lihu Road, Wuxi, 214122, China
[d] Jiangsu Provisional Research Center for Bioactive Product Processing Technology, Jiangnan University, 1800 Lihu Road, Wuxi, Jiangsu, 214122, China
[e] Key Laboratory of Plant Resource Conservation and Germplasm Innovation in Mountainous Region (Ministry of Education), College of Life Sciences/Institute of Agro-bioengineering, Guizhou University, Guiyang, 550025, China
[f] Dalian Research Institute of Petroleum and Petrochemicals, SINOPEC, Dalian, 116000, China
[g] School of Chemical Engineering, Dalian University of Technology, Dalian, 116000, China

ARTICLE INFO

Keywords:
Multiplex integration
Aspergillus niger
CRISPR-Cas9 homologous direct repair
White colony

ABSTRACT

Aspergillus niger is a highly versatile fungal strain utilized in industrial production. The expression levels of recombinant genes in *A. niger* can be enhanced by increasing the copy number. Nevertheless, given the prolonged gene editing cycle of *A. niger*, a "one-step" strategy facilitating the simultaneous integration of recombinant genes into multiple genomic loci would provide a definitive advantage. In our previous study, a visual multigene editing system (VMS) was designed to knock out five genes, employing a tRNA-sgRNA array that includes the pigment gene *albA* and the target genes. Building upon this system, hybrid donor DNAs (dDNAs) were introduced to establish a clustered regularly interspaced short palindromic repeats (CRISPR)-based multiplex integration toolkit. Firstly, a CRISPR-Cas9 homology-directed repair (CRISPR-HDR) system was constructed in *A. niger* by co-transforming the CRISPR-Cas9 plasmid (with a highly efficient sgRNA) and the dDNA, resulting in precise integration of recombinant xylanase gene *xynA* into the target loci (the β-glucosidase gene *bgl*, the amylase gene *amyA*, and the acid amylase gene *ammA*). Subsequently, the length of homology arms in the dDNA was optimized to achieve 100% editing efficiency at each of the three gene loci. To achieve efficient multiplex integration in *A. niger*, the CRISPR plasmid pLM2 carrying a sgRNA-tRNA array was employed for concurrent double-strand breaks at multiple loci (*bgl*, *amyA*, *ammA*, and *albA*). Hybrid dDNAs were then employed for repair, including dDNA1-3 (containing *xynA* expression cassettes without selection markers) and $dDNA_{albA}$ (for *albA* knockout). Among the obtained white colonies (RLM2′), 23.5% exhibited concurrent replacement of the *bgl*, *amyA*, and *ammA* genes with *xynA* (three copies). Notably, the xynA activity obtained by simultaneous insertion into three loci was 48.6% higher compared to that obtained by insertion into only the *bgl* locus. Furthermore, this multiple integration toolkit successfully enhanced the expression of endogenous pectinase pelA and *Candida antarctica* lipase CALB. Hence, the combined application of VMS and the CRISPR-HDR system enabled the simultaneous application of multiple selection markers, facilitating the rapid generation in the *A. niger* cell factories.

1. Introduction

As an important strain in industrial production, *Aspergillus niger* has been utilized to manufacture numerous products classified as Generally Regarded As Safe (GRAS), encompassing pharmaceutical proteins and enzyme preparations [1–3]. This fungus possesses many advantages, such as its efficient metabolic pathways and well-regulated gene networks, resulting in consistently high levels of protein expression (25–30 g/L) [2,4]. Moreover, *A. niger* can utilize cost-effective carbon sources like agricultural waste and plant substrates, which significantly

Peer review under responsibility of KeAi Communications Co., Ltd.
* Corresponding author. National Engineering Research Center for Cereal Fermentation and Food Biomanufacturing, Jiangnan University, Wuxi, 214122, China
E-mail address: liusong@jiangnan.edu.cn (S. Liu).

https://doi.org/10.1016/j.synbio.2024.01.014
Received 4 September 2023; Received in revised form 25 January 2024; Accepted 31 January 2024
Available online 10 February 2024
2405-805X/© 2024 The Authors. Publishing services by Elsevier B.V. on behalf of KeAi Communications Co. Ltd. This is an open access article under the CC BY-NC-ND license (http://creativecommons.org/licenses/by-nc-nd/4.0/).

decreases the cost of industrial-scale manufacturing [2]. Additionally, *A. niger* features a straightforward and readily scalable fermentation process, enabling high-density cultivation in large fermenters [5]. Hence, *A. niger* holds promising potential as a host cell in the production of high-value recombinant proteins; however, the expression levels of most proteins are limited.

To enhance the expression of recombinant proteins in *A. niger*, extensive screening and optimization of the promoters [6], 5′-untranslated regions [7,8], and open reading frames [9–11] have been meticulously conducted. In addition, increasing the copy number offers another avenue for boosting expression levels [2]. In wild-type (WT) *A. niger*, the remarkably efficient non-homologous end joining (NHEJ) mechanism enables the random insertion of a recombinant gene into the genome, resulting in the generation of multiple copies [2,12]. Nevertheless, the majority of genomic loci do not exhibit high transcription efficiency [13], and the inserted fragments may be lost during passaging, leading to unstable protein expression [14]. Therefore, targeted insertion of the recombinant gene into loci with efficient transcription can significantly enhance expression levels. Furthermore, a more advanced approach involving simultaneous integration at multiple high-expression loci could be established in *A. niger*.

Some clustered regularly interspaced short palindromic repeats (CRISPR)-mediated approaches have enabled the integration of foreign genes into the genome of *A. niger* [15–17]. However, editing multiple genes simultaneously remains challenging. For instance, utilizing the CRISPR-Cas9 homology-directed repair (CRISPR-HDR) system to concurrently insert glucose oxidase (*GoxC*) into the *glaA* and *amyA* gene loci of *A. niger* resulted in a 4-fold increase in GoxC activity [18]. However, each donor DNA (dDNA) carries a selection marker to enhance the efficiency. Therefore, the limited number of selection markers in *A. niger* constrains the application of this method for integrating genes into additional loci. To address this challenge, Mark et al. sequentially inserted the *glaA* expression cassette into predetermined sites in the *A. niger* genome, which demonstrated high efficiency in expressing starch-degrading enzymes. Subsequently, recombinant genes were knocked in at ten loci simultaneously by homologous recombination (HR) of marker-free dDNAs with the *glaA* expression cassette (promoter and terminator) [19]. Notably, the iterative insertion of the glaA expression cassette extended the overall process, highlighting the need for a multiplex integration method that requires fewer selection markers and involves shorter cycles.

In our previous research, a visual multigene editing system (VMS) was developed based on the pigment gene *albA*. A CRISPR plasmid containing a sgRNA-tRNA array was utilized to knock out four genes with an efficiency of up to 22% in the WT strain [20]. The capabilities of this method were further extended to facilitate multi-locus concurrent insertion. First, the CRISPR-HDR system was applied to replace the β-glucosidase gene *bgl*, the amylase gene *amyA*, and the acid amylase gene *ammA* with the recombinant xylanase gene (*xynA*). The sgRNA and homology arms were fine-tuned to optimize the integration efficiency. Finally, a CRISPR plasmid containing the sgRNA-tRNA array was employed along with hybrid dDNAs for insertions at multiple specific loci. Among them, the dDNA (containing hygromycin B, *hygB*) was utilized to disrupt *albA*, resulting in the generation of visually selectable white colonies as a screening marker, while other dDNAs did not require the selection marker. Moreover, endogenous pectate lyase (pelA) and *Candida antarctica* lipase B (CALB) were expressed in *A. niger* AG11 to demonstrate the universality of this toolkit in enhancing the expression of other enzymes. This method enabled multiplex integration in *A. niger*, thereby creating a high-expression host for industrial production.

2. Materials and methods

2.1. Strains and plasmids

Gene cloning was performed using *Escherichia coli* JM109 (Miaoling Bio, Wuhan, China) and plasmid pMD19 (Miaoling Bio, Wuhan, China). Enzyme expression was achieved by utilizing *A. niger* AG11 (CCTCC M2018881) and its derivatives, as displayed in Table S1.

2.2. Plasmid construction

XynA gene (GenBank: XM_001388485.2), *pelA* gene (GenBank: XP_001401061.1), and *CALB* gene (GenBank: Z30645.1) were separately cloned and seamlessly ligated with the P*bgl* (bgl promoter), the S*bgl* (bgl signal peptide), and the T*bgl* (bgl terminator) using the ClonExpress MultiS One Step Cloning Kit (Vazyme, Nanjing, China). The *hygB* expression cassette was efficiently assembled using the ClonExpress MultiS One-Step Cloning Kit with P*gpdA*, *hygB*, and *trpC*. Meanwhile, the dDNA constructs were engineered based on the pMD19 vector. Various lengths of homology arms were fused with the xynA expression cassette or the hygB expression cassette to improve the efficiency of CRISPR-HDR. Then, the specific primers were used to amplify the required fragments and obtain the dDNAs.

The CRISPR-Cas9 plasmids were constructed in a well-organized three-step process. Firstly, the sgRNA expression cassettes carrying P*u3**(mutated versions of U3 snRNA) and T*u3*, were seamlessly inserted into the pMD19 vector using the ClonExpress MultiS One Step Cloning Kit, yielding pMD19/sgRNA. Subsequently, linearization of pMD19/sgRNA was executed via specific primers that carried the 20 bp sgRNA, followed by transformation into *E. coli* JM109 to yield pMD19/sgRNA' with distinct sgRNA expression cassettes. Notably, various sgRNAs were selected as viable candidates using the CRISPOR software (https://crispor.tefor.net/crispor.py). Lastly, plasmids pFC330/pFC332 and pMD19/sgRNA' were linearized with SpeedyCut *PacI* and *BglII* (Sangon Biotech, Shanghai, China), and their fragments were circularized using DNA ligase solution I (TaKaRa, Dalian, China). The expression cassette containing multiple sgRNAs (tRNA-gRNA array) was described in our previous work [20]. The comprehensive lists of plasmids and primers used in this study are presented in detail in Table S1 and Table S2.

2.3. Construction of recombinant strains

The transformation and fermentation method of *A. niger* was performed following previously established protocols [12]. The total mass of CRISPR plasmids and mixed dDNAs for multiplex integration was maintained above 50 μg. Several white colonies were randomly selected from the colonies grown on high osmolarity czapek agar medium (34% sucrose, 0.3% $NaNO_3$, 0.05% KCl, 0.05% $MgSO_4{\cdot}7H_2O$, 0.001% $FeSO_4{\cdot}7H_2O$, 0.001% $ZnSO_4{\cdot}7H_2O$, 0.0005% $CuSO_4{\cdot}5H_2O$, and 0.5% agar), and the probabilities of *xynA* replacing *bgl*, *amyA*, and *ammA* in these white colonies were calculated. The genomic DNA was extracted using the DNAsecure kit (Tiangen Biotech, Shanghai, China). The schematic of gene sequence verification can be found in Fig. S1, and the designed primers used for the experiments are listed in Table S2.

2.4. qRT-PCR for quantification of the copy number

Mycelia were harvested from the fermentation culture at 24 h, and immediately cryogenically ground in liquid nitrogen. Total RNA was extracted from the mycelia using the RNAprep Pure Kit (Tiangen Biotech, Beijing, China) following the manufacturer's instructions, and eluted with RNase-free water. Subsequently, cDNA was synthesized from RNA using the PrimeScript™ RT-PCR Kit (Takara, Dalian, China). For quantitative PCR, a 96-well reaction plate was prepared using SYBRH Premix ExTaq™ (TaKaRa Biotechnology, Beijing, China). The cycling conditions were as follows: 95 °C for 30 s followed by 40 cycles of 95 °C for 5 s and 60 °C for 20 s. All reactions were performed on a LightCycler 480 II Real-time PCR instrument (Roche Applied Science, Mannheim, Germany). The cycle threshold (Ct) values were calculated on the PCR instrument software. The relative copy numbers were calculated as described in previous reports [21]. Additionally, the *actin*

gene was selected as an internal standard, and the primers used are presented in Table S2.

2.5. Determination of enzyme activity

The activity of xynA was assessed using the 3,5-dinitrosalicylic acid (DNS) method, as outlined in the study conducted by You et al. (2021) [22]. In this procedure, 900 μL of a 1% (w/v) solution of birchwood xylan (Sangon Biotech, Shanghai, China) was incubated with 100 μL of appropriately diluted enzyme solution at 50 °C for 10 min. The enzymatic reaction was halted by adding 2 mL of DNS reagent, followed by a 5 min incubation in a boiling water bath and subsequent cooling in water. The absorbance of the reaction solution was then measured at 545 nm using a BioTek Cytation 5 (Agilent, California, USA). Xylanase activity was quantified in units (U), representing the amount of enzyme required to produce 1 μmol of reducing sugar under the specified assay conditions (50 °C, pH 5.5). Similarly, the activity of pelA was determined using the DNS method [23]. Briefly, 50 μL of appropriately diluted enzyme solution was added to 450 μL of 0.1% polygalacturonic acid substrate (Tris-HCl, pH 7.0). The mixture was incubated at 40 °C for 30 min, and 500 μL DNS was added and boiled for 10 min. Finally, the solution was cooled to room temperature, and the absorbance at 540 nm was recorded. Enzyme activity was defined as the amount of enzyme that produced 1 μmol of D-galacturonic acid per minute under standard conditions.

The CALB activity assay method was performed according to methods from previous reports with some modifications [24]. The Tris-HCl buffer and 50 μL of appropriately diluted enzyme solution were mixed and preheated for 5 min. Subsequently, 50 μL of 25 mM *p*-nitrophenyl butyrate (pNPB) was added, and the reaction was allowed to proceed for 5 min. Finally, the reaction was terminated by adding pre-chilled ethanol. The absorbance of the reaction mixture was measured at 405 nm wavelength, with Tris-HCl buffer as a blank control. CALB activity was defined as the amount of enzyme required to generate 1 μmol of *p*-nitrophenol (pNP) per minute at 45 °C and pH 8.0.

2.6. Protein expression analysis

Protein analysis was conducted using SDS-PAGE on a 10% Bis-Tris protein gel (ThermoFisher Scientific, Shanghai, China) to assess the expression of enzymes. The protein bands were visualized using a Gel Doc imaging system (Bio-Rad, Hercules, USA) after staining with Coomassie Brilliant Blue R250 (Yeasen, Shanghai, China).

2.7. Statistical analysis

All experimental data were obtained independently with at least three replicates, and the results were presented as mean ± standard deviation. Differences between the two groups were assessed using a two-tailed Student's *t*-test. Statistical significance was denoted by * for $P < 0.05$ and ** for $P < 0.01$, respectively.

3. Results

3.1. Developing a CRISPR-HDR system for site-specific integration in A. niger

A CRISPR-Cas9 system was employed in combination with the dDNA to carry out site-specific insertion of the recombinant gene into the *A. niger* genome. The CRISPR-based plasmid (incorporating the Cas9 gene and the sgRNA expression cassette) was ingeniously engineered to facilitate the precise cleavage of target sequences in the genome, thereby enabling efficient integration of the dDNA through HR at the corresponding sites [18]. In our previous research, a proficient recombinant protein expressing locus (*bgl*) was uncovered in the *A. niger* AG11 strain [12]. In addition, genomic loci associated with high-expression proteins (glucoamylase glaA, amyA, and ammA) exhibited robust transcriptional capacity [13]. Therefore, these four loci were identified as potential integration sites for recombinant genes.

On the one hand, the utilization of starch as a carbon source relies on the presence of amylolytic enzymes to support cellular growth. On the other hand, the implementation of the CRISPR system in the knockout of the *glaA* gene in *A. niger* AG11 faced obstacles due to its low efficiency (data not shown). Therefore, *bgl*, *amyA*, and *ammA* were strategically selected as the integration sites for the recombinant gene *xynA*. Following the individual introduction of five CRISPR plasmids harboring distinct candidate sgRNA sequences (sgRNA1-sgRNA5) into the WT strain, the optimal $sgRNA_{bgl}$-4, $sgRNA_{amyA}$-1, and $sgRNA_{ammA}$-1 were determined based on the efficiency of target gene mutations (Fig. S2 and Table 1). Then, a co-transformation procedure was employed to introduce the pFC330 plasmid (harboring the sgRNA) (Fig. 1A) and the dDNA (encompassing 1500 bp homology arms along with the *xynA* and *hygB* expression cassettes) into the protoplasts to obtain the recombinant strain RL (Fig. 1B). The results revealed that the efficiency of *xynA* integration into the *bgl* locus, *amyA* locus, and *ammA* locus reached 75%, 80%, and 75%, respectively (Fig. 1D). Consequently, a CRISPR-HDR system enabling the insertion of a recombinant gene at each of three specific genomic loci was established in *A. niger* AG11.

3.2. Improvement of integration efficiency by optimizing homology arms

To enhance the efficiency of *xynA* integration into the specified loci, homology arms of length 2000 bp and 2500 bp were individually fused into dDNAs (Fig. 1C). The 2000 bp homology arms resulted in 100% insertion efficiency at the *amyA* and *ammA* loci, while the *bgl* locus required homology arms of 2500 bp in length to attain 100% insertion efficiency (Fig. 1D). Gene sequencing and SDS-PAGE analysis were conducted to confirm the complete replacement of these genes with *xynA* (Fig. S2). In summary, the homology arm lengths were refined and the integration efficiency of the recombinant gene using CRISPR-HDR reached 100% at the *bgl*, *amyA*, and *ammA* loci, respectively.

3.3. Construction of a visual multiplex integration toolkit in A. niger

Editing multiple genes in the *A. niger* genome is hindered by the lack of selection markers and the time-consuming gene manipulation [2,25]. In our previous study, one to five genes were knocked out by inserting diverse sgRNAs flanked with tRNAs into the CRISPR-Cas9 plasmid [20]. Building upon this strategy, the pLM1 plasmid was developed based on pFC330, which incorporated a tRNA-sgRNA array comprising three specific sgRNAs ($sgRNA_{bgl}$, $sgRNA_{amyA}$, and $sgRNA_{ammA}$) and three tRNAs ($tRNA_{Ala}$, $tRNA_{Phe}$, and $tRNA_{Arg}$) (Fig. 2A and Table S3). This engineered plasmid induced concurrent double-strand breaks (DSBs) in the *bgl*, *amyA*, and *ammA* genes within the ΔkusA strain (where NHEJ

Table 1
Optimization of sgRNAs in this study.

sgRNAs	Sequences (5′-3′)	Mutation efficiency (%)
$sgRNA_{bgl}$-1	TGCAGCAATACAACACTCTT	20
$sgRNA_{bgl}$-2	ACCGATATTGACTACATGCA	0
$sgRNA_{bgl}$-3	AAGTGGCGTTCGATGGTGTG	60
$sgRNA_{bgl}$-4	CACCCATCGTTTCTTCTCCC	80
$sgRNA_{bgl}$-5	TCTCACTTTTCGGCATTCCG	60
$sgRNA_{amyA}$-1	TCTCTTCGGCCCTTCATGAG	100
$sgRNA_{amyA}$-2	TACTCTCTGAACGAAAACTA	60
$sgRNA_{amyA}$-3	AAACTATGAAGATCAGACTC	0
$sgRNA_{amyA}$-4	CATATGGAGATGCCTACCAT	60
$sgRNA_{amyA}$-5	TTGTCCCTACCAGAACGTCA	60
$sgRNA_{ammA}$-1	CTGCCCCAGGATACTGCTGA	80
$sgRNA_{ammA}$-2	ATATCGTAGGCTTACTCTCA	60
$sgRNA_{ammA}$-3	TGCCCGCGGAATGTACCTCA	40
$sgRNA_{ammA}$-4	ATACTGCCTGATCACAGATT	0
$sgRNA_{ammA}$-5	CTCGGCCTACATTACCTACG	0

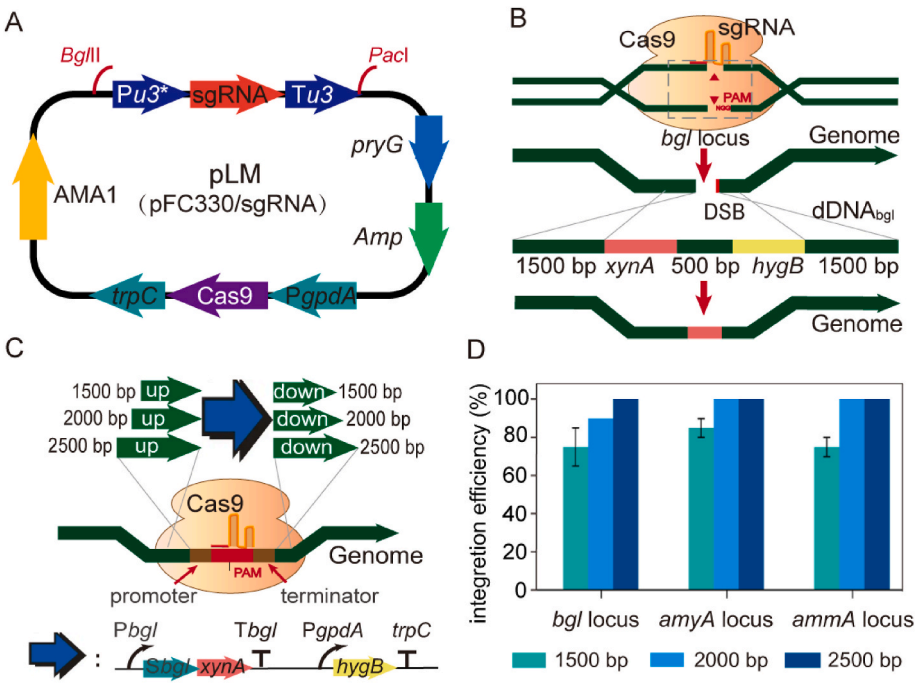

Fig. 1. Construction and optimization of the CRISPR-HDR system in *A. niger*. (A) Schematic diagram of the pFC330/sgRNA plasmid. The plasmid was constructed based on the pFC330 vector. The promoter and terminator of sgRNA were P*u3** (a mutant of P*u3*) [20] and T*u3*, respectively. In addition, the promoter P*gpdA* and terminator *trpC* were used to express Cas9 protein. (B) Schematic diagram of *xynA* insertion into the *bgl* locus using CRISPR-HDR. (C) Schematic diagram of the homology arm optimization to improve CRISPR-HDR efficiency. The promoter P*bgl,* signal peptide S*bgl,* and terminator T*bgl* were used to express xynA extracellularly. Meanwhile, the promoter P*gpdA* and terminator *trpC* were used to express hygB. (D) Effect of the homology arm length on integration efficiency at different loci.

was significantly inhibited) (Fig. 2B). Furthermore, $tRNA_{Ile}$ and $sgRNA_{albA}$ were incorporated into the tRNA-sgRNA array of pLM1 to construct the pLM2 plasmid, effectively producing white colonies as a visual marker (Fig. 2A and Table S3). These specific endogenous tRNAs have been proven to be highly effective in facilitating the release of sgRNA in *A. niger* AG11 [20]. In addition, mixed dDNAs were utilized to repair DSBs caused by the Cas9 protein in these loci (Fig. 2A and B). Among them, the pLM1 and selection marker-free dDNAs' (dDNA1, dDNA2, and dDNA3) enabled *xynA* to replace *bgl*, *amyA,* and *ammA*. In contrast, pLM2, dDNAs', and $dDNA_{albA}$ were used to obtain white colonies in which *xynA* replaced *bgl*, *amyA*, and *ammA* (Fig. 2B). Moreover, the selection marker *hygB* was incorporated into $dDNA_{albA}$ to increase the proportion of white colonies.

Notably, white colonies may be formed by HR of the $dDNA_{albA}$ with *albA* flanking sequences in the genome, obviating the necessity for Cas9 protein-mediated cleavage. The length of the homology arms in $dDNA_{albA}$ was optimized to ensure a significantly higher proportion of white colonies obtained through co-transformation of pLM3 (containing $sgRNA_{albA}$) and $dDNA_{albA}$ compared to transformation with $dDNA_{albA}$ alone (Fig. 3A). The largest difference in the white colony formation rate was observed between the co-transformation group (85%) and the transformation with $dDNA_{albA}$ alone group (5%) when employing 1000 bp homology arms (Fig. 3B). As a result, the lengths of homology arms in the dDNA1, dDNA2, dDNA3, and $dDNA_{albA}$ groups were set to 2500 bp, 2000 bp, 2000 bp, and 1000 bp, respectively (Fig. 2B). Finally, a CRISPR-mediated multiplex integration system was established by co-transforming the CRISPR-Cas9 plasmid (pLM1 or pLM2) and the hybrid dDNAs into the ΔkusA strain.

The black phenotyped strain RLM1 was obtained by transforming the pLM1 plasmid and dDNAs into the ΔkusA strain, and the probabilities of *bgl*, *amyA*, and *ammA* being replaced by *xynA* were determined to be 18.3%, 11.7%, and 10%, respectively (Fig. 2C and D). However, concurrent replacement of all three genes was observed in only 1.7% of the transformants (Fig. 2D). Nevertheless, RLM2 was generated by transforming the pLM2 plasmid and dDNAs into the ΔkusA strain, and 70% of the colonies (RLM2′) exhibited a white phenotype (Fig. 2C and Table S4). Then, the sequencing of the target gene in these white colonies demonstrated a notable increase in the site-specific integration efficiency of *xynA* (Table S4 and Fig. S3). Specifically, *xynA* replacing *bgl*, *amyA*, and *ammA* showed an efficiency of 74.5%, 56.9%, and 60.8%, respectively; the three genes were simultaneously replaced in 23.5% of the colonies in RLM2' (Fig. 2D). Hence, a pigment gene was included as a selection marker, increasing the proportion of colonies in which the recombinant genes integrated simultaneously into multiple loci. Furthermore, strains harboring four copies of *xynA* (comprising one endogenous copy and three integrated copies) demonstrated a remarkable 48.6% increase in xylanase activity (523 U/mL) compared to those derived from the sole substitution of the *bgl* gene with two copies of *xynA* (comprising one endogenous copy and one integrated copy) (Fig. S4). These findings indicate that augmenting the copy number of *xynA* at the high-expression site is an important factor in improving its expression.

Recombinant expression of the endogenous pelA and the *C. antarctica*-derived CALB was carried out to evaluate the system's generality in upregulating the expression of enzymes. Initially, genes *pelA* and *CALB* were individually integrated into the *bgl* locus, yielding recombinant strains RL/*pelA* and RL/*CALB* with copy numbers of 2 (including one endogenous copy) and 1, respectively. Utilizing the visual multiplex integration toolkit, approximately 25% of the white clones integrated the recombinant genes (*pelA*/*CALB*) into three loci simultaneously (Fig. S5A). The obtained recombinant strains RLM/*pelA* and RLM/*CALB* had copy numbers of 4 (including one endogenous copy) and 3, respectively. Moreover, their expression levels were 68% and 40.9% higher than RL/*pelA* and RL/*CALB*, respectively (Figure S5B and Figure S5C). Consequently, this integration system represents a valuable toolkit for augmenting the expression levels of recombinant proteins in *A. niger*.

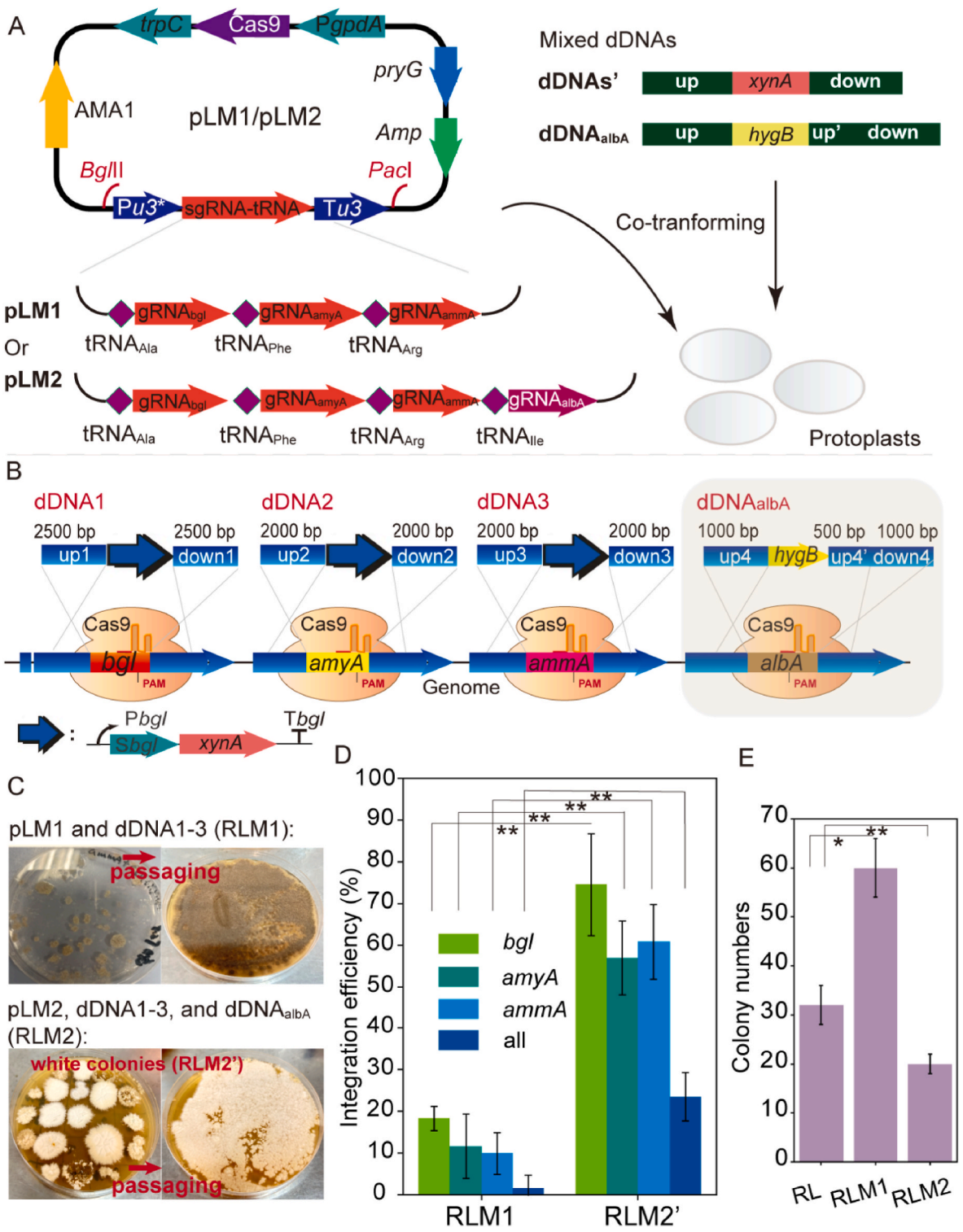

Fig. 2. CRISPR-HDR-mediated multiplex integration in *A. niger*. (A) Schematic of the CRISPR-HDR-mediated multiplex integration system. This system comprised a CRISPR plasmid with a Cas9 expression cassette, sgRNA-tRNA array, and mixed dDNAs. They were simultaneously introduced into the protoplasts of *A. niger* to facilitate multi-locus insertions in the genome. Notably, the pLM1 plasmid lacked $sgRNA_{albA}$, whereas it was present in pLM2. (B) Schematic of the dDNA repair of DSBs. The dDNAs underwent HR with the genomic fragments to integrate the xynA expression cassette into the genome. Specifically, dDNA1-dDNA3 was employed to integrate *xynA* at the *bgl*, *amyA*, and *ammA* loci, respectively; in contrast, $dDNA_{albA}$ induced the knockout of *albA*, resulting in the formation of white colonies. (C) The colony phenotype arose from two distinct strategies. RLM1 retained its unique production of black pigment, while in RLM2, 70% of the colonies (RLM2′) exhibited a white colony phenotype, which remained stable in subsequent passages. (D) The integration efficiency of *xynA* in RLM1 and RLM2'. In a randomly selected pool of 20 colonies, the ratio of positive colonies where the gene at a specific locus has been replaced by *xynA* represents the integration efficiency of *xynA* at that particular site. (E) The number of colonies. The strain RL was derived from the integration of *xynA* into a single locus. RLM1 was achieved via co-transformation involving plasmid pLM1 and dDNA1-3, whereas RLM2 was obtained through co-transformation with pLM2, dDNA1-3, and $dDNA_{albA}$. Differences were determined by a two-tailed Student's *t*-test. The * and ** indicate $P < 0.05$ and $P < 0.01$, respectively, and the error bars represent the standard deviation.

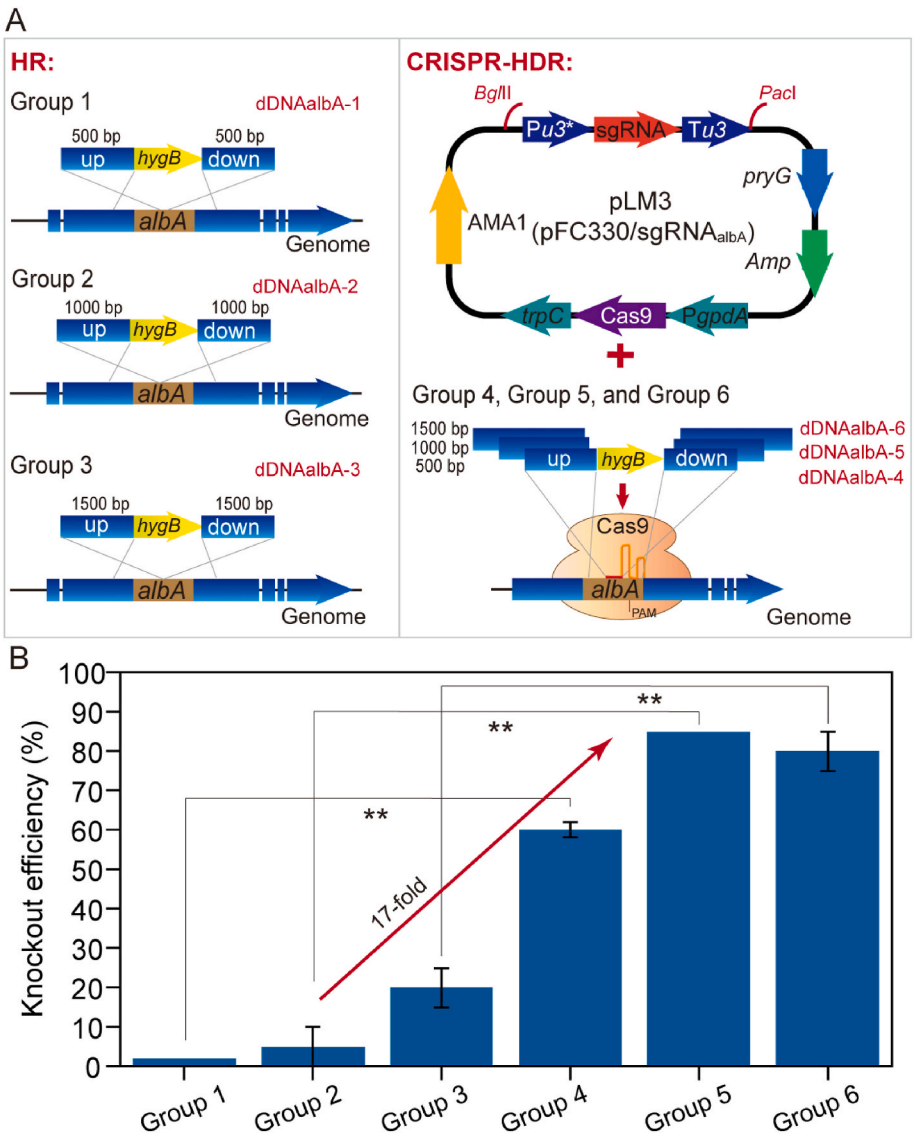

Fig. 3. Effect of the homology arm on the knockdown efficiency of *albA*. (A) Schematic of deleting *albA* using HR (different homology arms) (left) and CRISPR-HDR (different homology arms) (right), respectively. (B) Effect of different lengths of homology arms on the knockdown efficiency of *albA* using HR and CRISPR-HDR, respectively. Differences were determined by a two-tailed Student's *t*-test. The * and ** indicate $P < 0.05$ and $P < 0.01$, respectively, and the error bars represent the standard deviation.

4. Discussion

The copy number of the recombination gene in the genome can be enhanced through NHEJ; however, most randomly inserted loci do not exhibit high expression levels [2]. Due to the prolonged editing cycle and restricted availability of selection markers, accomplishing targeted integration at multiple high-expression sites remains a challenging task [18,19]. In this study, the efficiency of three sgRNAs ($sgRNA_{bgl}$, $sgRNA_{amyA}$, and $sgRNA_{ammA}$) was optimized by individually targeting insertion sites, thereby achieving integration efficiencies of over 80% in the ΔkusA strain. Meanwhile, the homology arms were adjusted to result in a 100% integration efficiency at the *bgl*, *amyA*, and *ammA* loci, respectively. Based on these, the established multiplex integration toolkit enabled a "one-step" insertion of *xynA* into the three sites, reducing the editing cycle from the original two months to two weeks. In addition, this method was successfully applied to separately integrate the endogenous pectinase gene *pelA* and exogenous lipase B gene *CALB* in the genome, effectively enhancing their copy numbers and expression levels, thereby demonstrating the universality of the integration system in *A. niger*. Notably, the CRISPR plasmid containing *pryG* was lost during the non-selective culture process, while the sole resistance selection marker *hygB* was eliminated during serial passaging (Fig. S6). The reintroduction of the pigment gene *albA* into the genome allowed for its reutilization as a selection marker, effectively addressing the constraints imposed by the limited selection markers in multiplex integration.

The multiplex integration strategy enables the construction of multi-enzyme expression systems, such as the rapid insertion of cellulase and hemicellulase genes into the genome of *A. niger*. In our upcoming research, the expression elements and insertion sites will be fine-tuned to customize the expression levels of different enzymes (glucanase, glucosidase, and xylanase), hence facilitating the utilization of *A. niger*'s fermentation broth for effective lignocellulosic degradation. Furthermore, the "one-step" incorporation of complete metabolic pathways into the *A. niger* genome enables the biosynthesis of target metabolites. Similar work has been carried out in yeast, where researchers have successfully synthesized 2,3-butanediol, β-carotene, zeaxanthin, and astaxanthin using a CRISPR-based synthetic biology toolkit (containing a series of sgRNA plasmids and donor plasmids) in *Pichia pastoris* [26]. In

summary, the CRISPR-based multiplex integration system allows *A. niger* to serve as a cell factory for the synthesis of recombinant proteins, natural products, and value-added chemicals.

The inclusion of the selection marker gene *hygB* in $dDNA_{ablA}$ increased the proportion of white colonies from 10% to 70% (data not shown), but also resulted in a threefold reduction in the total number of colonies compared to RLM1 (Fig. 2E). Meanwhile, the quantity of RLM2 colonies decreased by 50% compared to the RL strain, where recombinant genes integrate at a single locus (Fig. 2E). This reduction is attributed to the cytotoxicity caused by the failure to repair multiple DSBs simultaneously [27]. In addition, large homology arms (exceeding 1000 bp) were employed, which differs from the typical use of only a few dozen base pairs in other host systems [28–30]. Moreover, a concentration of 10 μg/μL hybrid dDNAs was used to facilitate the efficient repair of DSBs. Consequently, the insufficient HR efficiency in *A. niger* AG11 emerges as a limiting factor for the broader application of this multiplex integration method across more loci. Despite the observed significant reduction in NHEJ efficiency in the recombinant strain ΔkusA, an alternative strategy for enhancing HR involves the overexpression of homologous recombinase.

Besides achieving high HR efficiency, selecting easily editable integration sites is crucial for an efficient multiplex integration system. Our findings indicate that knocking out the highly expressed gene *glaA* in *A. niger* AG11 was particularly challenging (unpublished data), emphasizing the unsuitability of specific genomic loci as multigene integration targets. In *A. niger*, loci associated with glycoside hydrolases and proteases are the only viable insertion sites for recombinant genes that have been previously reported [18,19]. Currently, advanced methods such as droplet-based microfluidic systems and plasmid rescue strategies may facilitate the screening and identification of high expression loci within the *A. niger* genome [25,31]. Nevertheless, the editing challenges of these sites should be evaluated before inserting recombinant genes, minimizing the risk of compromising the overall efficiency of multiplex integration.

CRediT authorship contribution statement

Yangyang Li: Methodology, Investigation, Writing – original draft. **Cen Li:** Methodology, Resources. **Yishan Fu:** Methodology, Resources. **Quan Zhang:** Methodology, Resources. **Jianing Ma:** Methodology, Resources. **Jingwen Zhou:** Methodology, Resources, Writing – review & editing. **Jianghua Li:** Methodology, Resources, Writing – review & editing. **Guocheng Du:** Methodology, Resources, Writing – review & editing. **Song Liu:** Conceptualization, Writing – review & editing, Supervision, Project administration, Funding acquisition.

Declaration of competing interest

The authors declare that they have no known competing financial interests or personal relationships that could have appeared to influence the work reported in this paper.

Acknowledgments

This work was financially supported by the National Key Research and Development Program of China (2019YFA0706900), the National Natural Science Foundation of China (No. 32071474), and the Postgraduate Research and Practice Innovation Program of Jiangsu Province (KYCX20_1821).

Appendix A. Supplementary data

Supplementary data to this article can be found online at https://doi.org/10.1016/j.synbio.2024.01.014.

References

[1] Wang P, Xu S, Tang YQ, Wang H, Bai XL, Zhang HW. Genomic and AntiSMASH analyses of marine-sponge-derived strain *Aspergillus niger* L14 unveiling its vast potential of secondary metabolites biosynthesis. J. Fungi 2022;8(6):591.
[2] Li C, Zhou JW, Du GC, Chen J, Takahashi S, Liu S. Developing *Aspergillus niger* as a cell factory for food enzyme production, Biotechnol. Advisor 2020;44:107630.
[3] Ntana F, Mortensen UH, Sarazin C, Figge R. *Aspergillus*: a powerful protein production platform. Catalysts 2020;10(9):1400.
[4] Fiedler MRM, Barthel L, Kubisch C, Nai C, Meyer V. Construction of an improved *Aspergillus niger* platform for enhanced glucoamylase secretion. Microb Cell Factories 2018;17:95.
[5] Behera BC. Citric acid from *Aspergillus niger*: a comprehensive overview. Crit Rev Microbiol 2020;46(6):727–49.
[6] Li CH, Yan TR. Use of *Aspergillus niger* beta-glucosidase II gene (*bglII*) promoter elements to construct an efficient expression vector. J Taiwan Inst Chem Eng 2014;45(3):749–54.
[7] Hinnebusch AG, Ivanov IP, Sonenberg N. Translational control by 5 '-untranslated regions of eukaryotic mRNAs. Science 2016;352(6292):1413–6.
[8] Tamayo-Ramos JA, Barends S, de Lange D, de Jel A, Verhaert R, de Graaff L. Enhanced production of *Aspergillus niger* laccase-like multicopper oxidases through mRNA optimization of the glucoamylase expression system. Biotechnol Bioeng 2013;110(2):543–51.
[9] James ER, van Zyl WH, van Zyl PJ, Gorgens JF. Recombinant hepatitis B surface antigen production in *Aspergillus niger*: evaluating the strategy of gene fusion to native glucoamylase. Appl Microbiol Biotechnol 2012;96(2):385–94.
[10] Zhu SY, Xu Y, Yu XW. Improved homologous expression of the acidic lipase from *Aspergillus niger*. J Microbiol Biotechnol 2020;30(2):196–205.
[11] Rojas-Sanchez U, Lopez-Calleja AC, Millan-Chiu BE, Fernandez F, Loske AM, Gomez-Lim MA. Enhancing the yield of human erythropoietin in *Aspergillus niger* by introns and CRISPR-Cas9, Protein Expr. Purif 2020;168:105570.
[12] Li YY, Li C, Aqeel SM, Wang YC. Enhanced expression of xylanase in *Aspergillus niger* enabling a two-step enzymatic pathway for extracting β-glucan from oat bran. Bioresour Technol 2023;377:128962.
[13] Lubertozzi D, Keasling JD. Developing *Aspergillus* as a host for heterologous expression, Biotechnol. Advisor 2009;27(1):53–75.
[14] Zhang JX, Mao ZH, Xue W, Li Y, Tang GM, Wang AQ, Zhang YJ, Wang HM. Ku80 gene is related to non-homologous end-joining and genome stability in *Aspergillus niger*. Curr Microbiol 2011;62(4):1342–6.
[15] Zeng X, Zheng JW, Lu FF, Pan L, Wang B. Heterologous synthesis of Monacolin J by reconstructing its biosynthetic gene cluster in *Aspergillus niger*. J. Fungi 2022;8(4):407.
[16] Jin FJ, Wang BT, Wang ZD, Jin L, Han P. CRISPR/Cas9-based genome editing and its application in *Aspergillus* species. J. Fungi 2022;8(5):467.
[17] Zhang Y, Ouyang LM, Nan YL, Chu J. Efficient gene deletion and replacement in *Aspergillus niger* by modified in vivo CRISPR/Cas9 systems, Bioresour. Bioprocess 2019;6:4.
[18] Dong HZ, Zheng JW, Yu D, Wang B, Pan L. Efficient genome editing in *Aspergillus niger* with an improved recyclable CRISPR-HDR toolbox and its application in introducing multiple copies of heterologous genes. J Microbiol Methods 2019;163:105655.
[19] Arentshorst M, Valappil PK, Mozsik L, Regensburg-Tuink TJG, Seekles SJ, Tjallinks G, Fraaije MW, Visser J, Ram AFJ. A CRISPR/Cas9-based multicopy integration system for protein production in *Aspergillus niger*. FEBS J 2023;290(21):5127–40.
[20] Li C, Zhou JW, Rao SQ, Du GC, Liu S. Visualized multigene editing system for *Aspergillus niger*. ACS Synth Biol 2021;10(10):2607–16.
[21] Ziemons S, Koutsantas K, Becker K, Dahlmann T, Kuck U. Penicillin production in industrial strain P2niaD18 is not dependent on the copy number of biosynthesis genes. BMC Biotechnol 2017;17:16.
[22] You S, Zha ZQ, Li J, Zhang WX, Bai ZY, Hu YH, Wang X, Chen YW, Chen ZL, Wang J, Luo HY. Improvement of XYL10C_Delta N catalytic performance through loop engineering for lignocellulosic biomass utilization in feed and fuel industries. Biotechnol Biofuels 2021;14(1):195.
[23] Lin JF, Xiang SW, Lv H, Wang TT, Rao YL, Liu L, Yuan DZ, Wang XR, Chu YW, Luo D, Song T. Antimicrobial high molecular weight pectin polysaccharides production from diverse citrus peels using a novel PL10 family pectate lyase. Int J Biol Macromol 2023;234:123457.
[24] Liu ZQ, Zheng XB, Zhang SP, Zheng YG. Cloning, expression and characterization of a lipase gene from the ZJB09193 and its application in biosynthesis of vitamin A esters. Microbiol Res 2012;167(8):452–60.
[25] Li QH, Lu JC, Zhang GQ, Liu S, Zhou JW, Du GC, Chen J. Recent advances in the development of *Aspergillus* for protein production, Bioresour. Technol 2022;348:126768.
[26] Gao JC, Xu JH, Zuo YM, Ye CF, Jiang LJ, Feng LJ, Huang L, Xu ZN, Lian JZ. Synthetic biology toolkit for marker-less integration of multigene pathways into *Pichia pastoris* via CRISPR/Cas9. ACS Synth Biol 2022;11(2):623–33.
[27] Ganesan V, Monteiro L, Pedada D, Stohr A, Blenner M. High-efficiency multiplexed cytosine base editors for natural product synthesis in *Yarrowia lipolytica*. ACS Synth Biol 2023;12(10):3082–91.
[28] Weninger A, Fischer JE, Raschmanová H, Kniely C, Vogl T, Glieder A. Expanding the CRISPR/Cas9 toolkit for with efficient donor integration and alternative resistance markers. J Cell Biochem 2018;119(4):3183–98.

[29] Mund M, Weber W, Degreif D, Schiklenk C. A MAD7-based genome editing system for *Escherichia coli*, Microb. Biotechnol 2023;16(5):1000–10.
[30] DiCarlo JE, Norville JE, Mali P, Rios X, Aach J, Church GM. Genome engineering in *Saccharomyces cerevisiae* using CRISPR-Cas systems. Nucleic Acids Res 2013;41(7):4336–43.
[31] Qin LN, Jiang XZ, Dong ZY, Huang JZ, Chen XZ. Identification of two integration sites in favor of transgene expression in *Trichoderma reesei*, Biotechnol. Biofuels 2018;11:142.